Supplementary Information for Large-scale simulations of vortex Majorana zero modes in topological crystalline insulators

Chun Yu Wan[1], Yujun Zhao[1], Yaoyi Li[2,3,4], Jinfeng Jia[2,3,4,5,6], Junwei Liu[1*]

[1]Department of Physics, Hong Kong University of Science and Technology, Clear Water Bay, Hong Kong, China.
[2]Key Laboratory of Artificial Structures and Quantum Control (Ministry of Education), Tsung-Dao Lee Institute, School of Physics and Astronomy, Shanghai Jiao Tong University, Shanghai, 200240, China.
[3]Hefei National Laboratory, Hefei, 230088, China.
[4]Shanghai Research Center for Quantum Sciences, Shanghai, 201315, China.
[5]Southern University of Science and Technology, Shenzhen, 518055, China.
[6]Quantum Science Center of Guangdong-Hong Kong-Macao Greater Bay Area (Guangdong), Shenzhen, 518045, China.

*Corresponding author(s). E-mail(s): liuj@ust.hk;

This PDF file includes:
Supplementary Text
Figs. S1-S3
Supplementary references

S1 Symmetry operators for the tight-binding model

The symmetry operators for the BdG Hamiltonian of a vortex line (eq. 14 in the main text) can be decomposed into 5 parts

$$O_{\text{vortex}} = O_{\text{ph}} \otimes O_{x,y} \otimes O_z \otimes O_{\text{orb}} \otimes O_{\text{spin}}. \tag{1}$$

O_{ph} is in the Nambu basis. O_{xy} and O_z are for the sites in the supercell for the vortex line, $z = 0, 1$ since there are 2 sublattices. O_{orb} is for orbitals p_x, p_y and p_z. O_{spin} is for the spin basis.

The particle-hole symmetry operator is

$$C_{\text{ph}} = \begin{pmatrix} 0 & K \\ K & 0 \end{pmatrix}, \tag{2}$$

where K is the complex conjugation operator. The Hamiltonian satisfies $CH_{\text{BdG}}(k_z)C^{-1} = -H_{\text{BdG}}(-k_z)$ with $C^2 = +1$.

The magnetic mirror symmetry $M_T = M_{1\bar{1}0}T$ is written as

$$M_T = \begin{pmatrix} e^{i\pi/4} i\sigma_y m_{1\bar{1}0} K & 0 \\ 0 & e^{-i\pi/4} i\sigma_y m^*_{1\bar{1}0} K \end{pmatrix}, \tag{3}$$

where σ_y is a Pauli matrix in the spin basis. The phase factors $e^{\pm i\pi/4}$ are introduced to cancel the phases generated when rotating the vortex [1]. And $m_{1\bar{1}0}$ is the mirror symmetry operator for the band Hamiltonian

$$m_{1\bar{1}0} = m^{(xy)}_{1\bar{1}0} \otimes \mathbb{I}_2 \otimes \begin{pmatrix} 0 & 1 & 0 \\ 1 & 0 & 0 \\ 0 & 0 & 1 \end{pmatrix} \otimes \frac{i}{\sqrt{2}} (\sigma_x - \sigma_y), \tag{4}$$

where $m^{(xy)}_{1\bar{1}0}$ transforms (x, y) to (y, x) and $\mathbb{I}_2$ is an identity in the z basis. And the origin $(0, 0)$ is the center of the lattice.

The Hamiltonian satisfies $M_T H_{\text{BdG}}(k_z) M_T^{-1} = H_{BdG}(-k_z)$ with $M_T^2 = +1$, it acts as an effective time-reversal symmetry. A chiral symmetry operator can be defined by $\Gamma = CM_T$, The Hamiltonian satisfies $\Gamma H_{\text{BdG}}(k_z)\Gamma^{-1} = -H_{\text{BdG}}(k_z)$ with $\Gamma^2 = +1$ [2–4]. In this case the 1D vortex line in SnTe belongs to Altland-Zirnbauer class BDI with a topological invariant of integer values [2, 5].

For even N_x and N_y, the system preserves nonsymmorphic symmetries that interchange the sublattices [6]. The magnetic glide symmetry $G_T = G_y T$ is written as

$$G_T = \begin{pmatrix} i\sigma_y g_y(k_z) K & 0 \\ 0 & i\sigma_y g^*_y(-k_z) K \end{pmatrix}, \tag{5}$$

$$g_y = g^{(xy)}_y \otimes \begin{pmatrix} 0 & e^{-ik_z a/2} \\ e^{ik_z a/2} & 0 \end{pmatrix} \otimes \begin{pmatrix} 1 & 0 & 0 \\ 0 & -1 & 0 \\ 0 & 0 & 1 \end{pmatrix} \otimes (-i\sigma_y) \tag{6}$$

and $g_y^{(xy)}$ transforms (x, y) to $(x, -y)$. And $G_T^2 = -1$ at $k_z = -\pi/a$ guarantees a Kramers degeneracy for the vortex line.

And the screw symmetry operator S_{4z} is written as

$$S_{4z} = \begin{pmatrix} e^{i\pi/4} s_{4z}(k_z) & 0 \\ 0 & e^{-i\pi/4} s_{4z}^*(-k_z) K \end{pmatrix}, \tag{7}$$

$$\begin{aligned} s_{4z} = s_{4z}^{(xy)} \otimes \begin{pmatrix} 0 & e^{ik_z a/2} \\ e^{-ik_z a/2} & 0 \end{pmatrix} \otimes \begin{pmatrix} 0 & -1 & 0 \\ 1 & 0 & 0 \\ 0 & 0 & 1 \end{pmatrix} \\ \otimes \frac{1}{\sqrt{2}} (\sigma_0 - i\sigma_z) \end{aligned} \tag{8}$$

and $s_{4z}^{(xy)}$ transforms (x, y) to $(-y, x)$.

S2 Recursive Green's Functions

We use recursive Green's functions [7] to calculate the number of zero-energy states near the surface. The LDOS $d^i(E)$ is defined in Eq. 3 of the main text. We calculate the number of zero-energy states by integrating the LDOS using η smaller than the lowest nonzero eigenenergy. We checked that for our choice of parameters we can use $\eta = 10^{-6}$, and $d^i(E)$ can be described by a single Lorentz function.

$$d^i(E) \approx \frac{1}{\pi} \sum_{E_k = 0} \langle i|k\rangle\langle k|i\rangle \frac{\eta}{(E - E_k)^2 + \eta^2}. \tag{9}$$

The energy integration can be replaced by $\pi\eta d^i(E = 0)$.

Since the Hamiltonian has no z dependence, the surface Green's functions can be obtained recursively [7]. And we define the LDOS for each layer at zero energy as $D(z)$. We iterate the surface Green's functions to obtain the LDOS for n_z layers below the surface. Then the number of MZMs can be approximated by

$$N = \sum_{z=1}^{n_z} D(z), \tag{10}$$

the results are shown in Fig. 4(b) in the main text using $n_z = 100, 200$. In Fig. S1 we show $D(z)$ for some values of (μ, E_Z). Near the phase transition points the MZMs penetrate too deep inside the bulk [8, 9], and N deviates from an integer value [e.g., Fig. 4(b) in the main text].

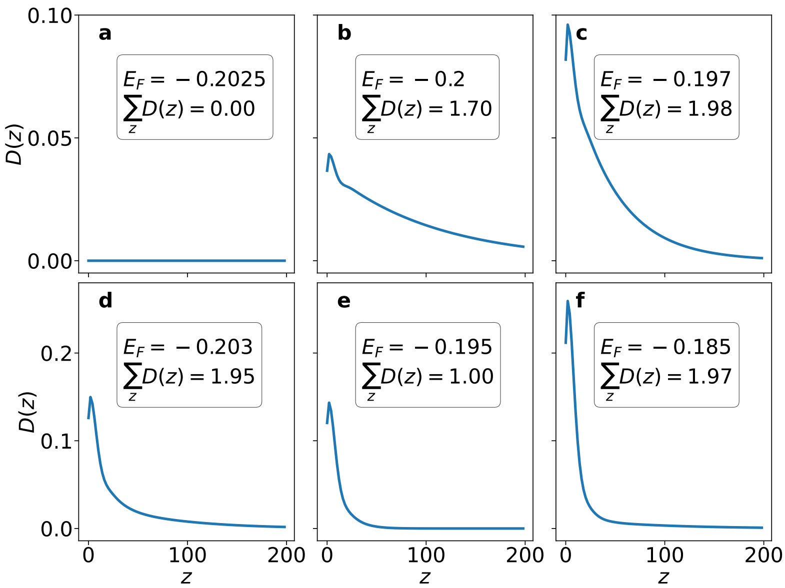

Fig. S1 Distribution of the MZMs $D(z)$ for the top $n_z = 200$ layers. Zeeman energy $E_Z = 0$ in (a-c) and $E_Z = 0.015$ in (d-f). $E_F = \mu - E_D$ as defined in the main text.

S3 Winding number

The number of MZMs is equal to the winding number

$$\nu = \frac{1}{2\pi} \int_0^{2\pi} d\theta(k_z), \tag{11}$$

where $\theta(k_z)$ is the angle of the $\boldsymbol{d}$ vector in Nambu space. For a vortex line, the winding number is generalized to include other degrees of freedom (sites, spins, orbitals, etc.), which is defined as [5, 10, 11]

$$\nu = \frac{1}{4\pi i} \int_0^{2\pi} dk_z \mathrm{Tr}\left[\Gamma \frac{H_{BdG}(k_z)}{dk_z} H_{BdG}^{-1}(k_z)\right]. \tag{12}$$

We show the integrands for some values of (μ, E_Z) in Fig. S2. Previous references for vortex phase transitions only calculated the crossing of vortex line to deduce the change of the number of MZMs, which leads to ambiguous results when the system preserves a chiral symmetry that supports multiple MZMs. In Fig. S2 (d-f), we explicitly show that ν changes as $2 \to 1 \to 2$, and the result is consistent with the number of MZMs at each end obtained in the last section.

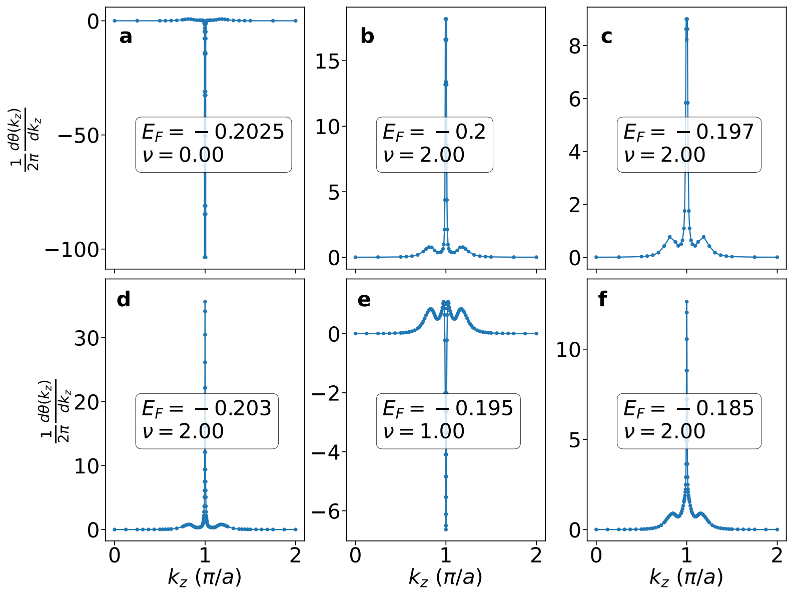

Fig. S2 The integrands of the winding number. Zeeman energy $E_Z = 0$ in (a-c) and $E_Z = 0.015$ in (d-f).

S4 Vortex phase transitions for odd $N_x = N_y$

In the main text we have shown that the single MZM phase may appears between vortex phase transitions if G_T is broken, and confirmed it using an in-plane Zeeman field that breaks G_T. In Fig. S3 we show $\nu = 1$ can also be realized in system with odd $N_x = N_y$ that breaks G_T. The calculations are the same as those for Fig. 4 in the main text, except that in Fig. S3 (d-g) we show the C_{4z} eigenvalues since S_{4z} is broken.

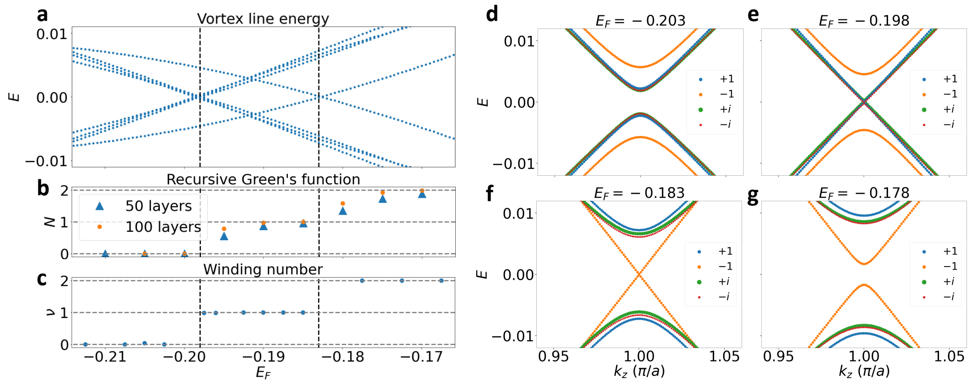

Fig. S3 Vortex phase transition in SnTe under an out-of-plane magnetic field. (a) The vortex line energy at $k_z = \pi/a$, it can be non-degenerate since G_T is broken. The number of MZMs are calculated using recursive Green's functions (b) and winding number (c). The black dashed lines denote crossings at $k_z = \pi/a$. (d-g) Vortex line energy for different k_z, the colors denote the C_{4z} eigenvalues. We use $\Delta_0 = 0.1$, $\xi_0 = 1$ for the vortex and $N_x = N_y = 21$ for the lattice.

References

[1] S. Qin, L. Hu, C. Le, J. Zeng, F.c. Zhang, C. Fang, J. Hu, Quasi-1d topological nodal vortex line phase in doped superconducting 3d dirac semimetals. Physical Review Letters **123**(2), 027003 (2019)

[2] A.P. Schnyder, S. Ryu, A. Furusaki, A.W. Ludwig, Classification of topological insulators and superconductors in three spatial dimensions. Physical Review B **78**(19), 195125 (2008)

[3] C.K. Chiu, J.C. Teo, A.P. Schnyder, S. Ryu, Classification of topological quantum matter with symmetries. Reviews of Modern Physics **88**(3), 035005 (2016)

[4] Y. Xiong, A. Yamakage, S. Kobayashi, M. Sato, Y. Tanaka, Anisotropic magnetic responses of topological crystalline superconductors. Crystals **7**(2), 58 (2017)

[5] S. Tewari, J.D. Sau, Topological invariants for spin-orbit coupled superconductor nanowires. Physical Review Letters **109**(15), 150408 (2012)

[6] S. Kobayashi, S. Sumita, M. Hirayama, A. Furusaki, Crystal-symmetry-protected gapless vortex-line phases in superconducting Dirac semimetals. Physical Review B **107**(21), 214518 (2023)

[7] M.L. Sancho, J.L. Sancho, J.L. Sancho, J. Rubio, Highly convergent schemes for the calculation of bulk and surface Green functions. Journal of Physics F: Metal Physics **15**(4), 851 (1985)

[8] Z.Z. Li, F.C. Zhang, Q.H. Wang, Majorana modes in a topological insulator/s-wave superconductor heterostructure. Scientific Reports **4**(1), 1–6 (2014)

[9] T. Kawakami, X. Hu, Evolution of density of states and a spin-resolved checkerboard-type pattern associated with the Majorana bound state. Physical Review Letters **115**(17), 177001 (2015)

[10] M. Sato, S. Fujimoto, Majorana fermions and topology in superconductors. Journal of the Physical Society of Japan **85**(7), 072001 (2016)

[11] S. Kobayashi, A. Furusaki, Double Majorana vortex zero modes in superconducting topological crystalline insulators with surface rotation anomaly. Physical Review B **102**(18), 180505 (2020)